

# Advanced Cardiac MRI Techniques for Evaluation of Left-Sided Valvular Heart Disease

Carmen P.S. Blanken, MS,<sup>1</sup> Emile S. Farag, MD,<sup>2</sup> S. Matthijs Boekholdt, MD, PhD,<sup>3</sup>  
 Tim Leiner, MD, PhD,<sup>4</sup> Jolanda Kluin, MD, PhD,<sup>2</sup> Aart J. Nederveen, PhD,<sup>1</sup>  
 Pim van Ooij, PhD,<sup>1</sup> and R. Nils Planken, MD, PhD<sup>1\*</sup>

The most common types of left-sided valvular heart disease (VHD) in the Western world are aortic valve stenosis, aortic valve regurgitation, and mitral valve regurgitation. Comprehensive clinical evaluation entails both hemodynamic analysis and structural as well as functional characterization of the left ventricle. Cardiac magnetic resonance imaging (MRI) is an established diagnostic modality for assessment of left-sided VHD and is progressively gaining ground in modern-day clinical practice. Detailed flow visualization and quantification of flow-related biomarkers in VHD can be obtained using 4D flow MRI, an imaging technique capable of measuring blood flow in three orthogonal directions over time. In addition, recent MRI sequences enable myocardial tissue characterization and strain analysis. In this review we discuss the emerging potential of state-of-the-art MRI including 4D flow MRI, tissue mapping, and strain quantification for the diagnosis and prognosis of left-sided VHD.

**Level of Evidence:** 1

**Technical Efficacy Stage:** 1

**J. MAGN. RESON. IMAGING 2018;48:318–329.**

Cardiac magnetic resonance imaging (MRI) and echocardiography are noninvasive imaging modalities that are of paramount importance in daily clinical practice for diagnosis, prognosis, and treatment planning in patients with left-sided valvular heart disease (VHD).<sup>1–3</sup> The most common types of left-sided VHD in the Western world are aortic valve stenosis (AS), aortic valve regurgitation (AR), and mitral valve regurgitation (MVR), with estimated prevalences of 0.4%, 0.5%, and 1.7%, respectively.<sup>4</sup> AS is most often caused by degenerative calcification of the aortic valve leaflets, whereas AR can result from valve stiffening due to calcification, but can also result from aortic valve endocarditis or aortic annulus dilatation.<sup>5</sup> MVR is generally divided into two categories: primary organic MVR, which occurs as a result of an intrinsically abnormal mitral valve, and functional MVR, which develops secondary to left ventricular

(LV) dysfunction or annular dilatation prohibiting normal valve closure.<sup>6</sup> AS, AR, and MVR may all lead to LV remodeling and eventually heart failure due to LV pressure and/or volume overload.

Cardiac MRI is the standard of reference for the quantification of ventricular volumes, mass, and function and is a highly valuable and reproducible tool in the diagnostic armamentarium for VHD.<sup>1,7</sup> Images are typically obtained using time-resolved (cine) MRI techniques, allowing targeted imaging of all heart valves and myocardial structures during the cardiac cycle. Furthermore, MR angiography (MRA) allows for assessment of large vessels like the aorta, with or without the use of contrast agents. However, to investigate which hemodynamic mechanisms drive disease progression in VHD, 3D evaluation of flow patterns is indispensable, as 2D imaging does not fully capture complex blood flow.

View this article online at [wileyonlinelibrary.com](http://wileyonlinelibrary.com). DOI: 10.1002/jmri.26204

Received Feb 14, 2018, Accepted for publication Apr 19, 2018.

The first two authors contributed equally to this work.

\*Address reprint requests to: R.N.P., Meibergdreef 9, 1105 AZ Amsterdam, the Netherlands. E-mail: [r.n.planken@amc.uva.nl](mailto:r.n.planken@amc.uva.nl)

From the <sup>1</sup>Department of Radiology and Nuclear Medicine, Academic Medical Center, Amsterdam, the Netherlands; <sup>2</sup>Department of Cardiothoracic Surgery, Academic Medical Center, Amsterdam, the Netherlands; <sup>3</sup>Department of Cardiology, Academic Medical Center, Amsterdam, the Netherlands; and <sup>4</sup>Department of Radiology, University Medical Center, Utrecht, the Netherlands

This is an open access article under the terms of the Creative Commons Attribution NonCommercial License, which permits use, distribution and reproduction in any medium, provided the original work is properly cited and is not used for commercial purposes.

Four-dimensional flow MRI (4D flow MRI or time-resolved 3D phase-contrast MRI with three-directional velocity encoding) is an imaging modality capable of measuring blood flow in the three principal directions and as a function of time, allowing for accurate quantification of blood flow in patients with VHD. An example acquisition protocol for cardiac MRI including 4D flow MRI can be found in Allen et al.<sup>8</sup> 4D flow MRI-derived parameters, such as wall shear stress and kinetic energy, enable characterization of hemodynamic mechanisms in patients with left-sided VHD. In addition, tissue characterization techniques such as  $T_1$ - and  $T_2$ -mapping enable quantification of myocardial fibrosis, extracellular volume (ECV) fraction, and edema, which can be used to study the effects of VHD on the myocardium. Strain analysis provides functional information regarding the contractility of the heart, facilitating timely identification of myocardial dysfunction.<sup>9</sup> Thus, novel state-of-the-art cardiac MRI techniques include 4D flow MRI, tissue characterization mapping, and strain quantification.<sup>8</sup>

In this review we provide a comprehensive overview of advanced MRI techniques for the evaluation of left-sided VHD. Current clinical imaging techniques (echocardiography and MRI) are discussed, followed by an overview of novel hemodynamic parameters derived from 4D flow MRI and their diagnostic and prognostic potential. Finally, we discuss the role of tissue mapping and strain quantification in left-sided VHD.

## Current Clinical Diagnostic Tools

### Echocardiography

Current clinical guidelines recommend transthoracic echocardiography (TTE) or transesophageal echocardiography (TEE) as the first-line diagnostic modality for the evaluation of left-sided VHD.<sup>1</sup> TTE is relatively cheap, fast, noninvasive, and can be performed in real time at the bedside to acquire relevant information on valve function and anatomy. Furthermore, cardiac blood flow assessment is possible using the color Doppler mode. In AS patients, echocardiography is used to assess aortic valve morphology, as well as several parameters to grade AS severity including peak systolic blood flow velocities and derivatives such as transvalvular pressure gradients and the aortic valve area (AVA).<sup>1</sup> In AR, it is used to assess valve morphology and the direction and severity of the regurgitation jet.<sup>1</sup> Quantification of AR can be performed by measuring the regurgitation fraction, but is typically performed taking into account a variety of parameters such as LV dilatation, the width of the regurgitant jet (vena contracta width), pressure half-time, and the presence of flow reversal in the descending aorta. In patients with MVR, echocardiography is useful to discriminate organic from functional MVR. Assessment of MVR severity is based on a range of qualitative and semiquantitative measures, including valve morphology

and movement, LV dilatation and function, left atrial dilatation, effective regurgitant orifice area, vena contracta width, flow reversal in the pulmonary veins, and pulmonary artery pressure.<sup>1,10</sup>

One of the main limitations of routine 2D echocardiography for hemodynamic assessment is that, due to the assumption of a circular geometry of the flow pattern, the complex dynamic nature of the blood flow tends to be overlooked. As a result, quantification of transvalvular flow is challenging and possibly inaccurate. Also, echocardiography can only measure velocities in line with the transducer beam, making it susceptible to errors caused by misalignment of the transducer beam to the direction of the blood flow, especially for eccentric and dynamic flow jets.<sup>11,12</sup> Furthermore, the complex geometry and dynamic nature of the valve apparatus during the cardiac cycle are not fully captured. Although 3D echocardiography enables more comprehensive, volumetric imaging of the heart, spatial and temporal resolutions are poorer and its clinical applicability is limited due to the significant learning curve.<sup>13</sup>

### Current Clinical Cardiac MRI

MRI is becoming increasingly important in the assessment of left-sided VHD in addition to echocardiography, providing accurate information on functional and morphological valvular abnormalities, VHD severity, and LV function. Recent clinical guidelines recommend MRI as an alternative for inconclusive TTE examinations, caused by poor acoustic windows, for instance.<sup>1,14</sup> Using steady-state free-precession (SSFP) imaging and accurate adjustment of imaging planes, all four heart valves can be visualized in predefined imaging planes.<sup>3</sup> 2D phase-contrast velocity mapping enables quantification of blood flow volumes and velocities across heart valves. However, slice-based cine imaging for the assessment of AS, AR, or MVR relies on correct manual plane positioning and angulation. In addition, imaging in a fixed plane does not allow for accurate assessment of dynamic cardiac structures, which is particularly relevant for the atrioventricular valves. Thus, although MRI is considered more accurate and reproducible than echocardiography in the assessment of ventricular volumes and flow across the heart valves,<sup>15,16</sup> obtaining a correct understanding of valvular function based on 2D imaging remains a challenge. The most important advantages and disadvantages of cardiac MRI and echocardiography for the quantitative assessment of VHD are summarized in a publication by Thavendiranathan et al.<sup>13</sup>

### 4D Flow MRI

4D flow MRI, or time-resolved 3D phase-contrast MRI, is powerful in its capability to noninvasively measure blood flow velocities in vivo within a volume in the three principal directions. It allows for the dynamic quantification of blood flow in both the heart and the great vessels with good spatial and

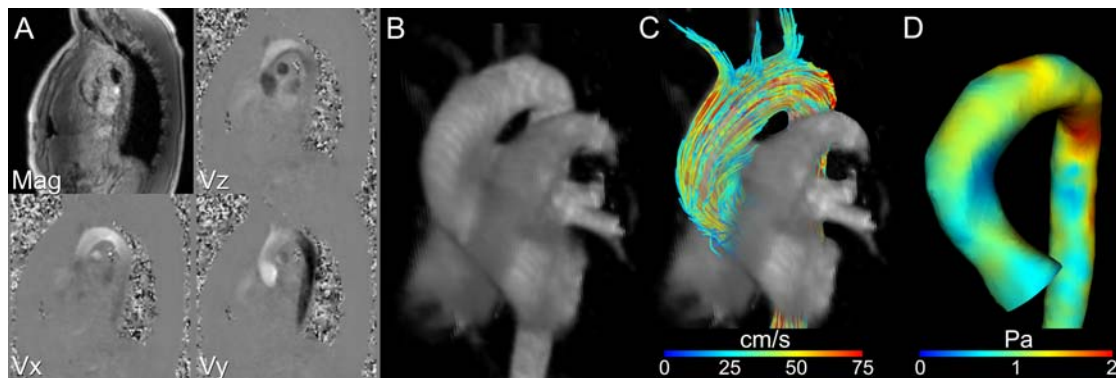


**FIGURE 1:** (A) Thoracic 4D flow MRI acquisition consisting of magnitude (Mag) and velocity data in three orthogonal directions (Vx, Vy, and Vz), (B) phase-contrast MRA, (C) systolic pathline visualization of the thoracic aorta, color-coded for velocity, and (D) systolic wall shear stress visualization.

temporal resolutions. Pathline or streamline visualizations provide insight into 3D hemodynamics and 4D flow MRI-derived hemodynamic parameters may aid in the evaluation of VHD (Fig. 1). Scan times range from 5–10 minutes with the use of advanced acceleration techniques and respiratory motion is usually compensated for with navigator gating at the lung–liver interface or a respiratory belt. Recommended acquisition parameters have been stated by Dyverfeldt et al.<sup>17</sup>

In 4D flow MRI, velocity data are acquired in an entire volume of interest, enabling blood flow quantification during postprocessing in any desired orientation. Consequently, 4D flow MRI is better suited for visualization and quantification of eccentric and dynamic transvalvular flow patterns than 2D PC-MRI.<sup>18,19</sup> Valve orifice areas and pressure gradients can be calculated from peak flow velocities using the simplified Bernoulli equation.<sup>20</sup> 4D flow MRI in combination with valve tracking offers the possibility to quantify transvalvular blood flow corrected for cardiac motion, and has been shown to yield good correlations across heart valves.<sup>21–23</sup> Dedicated software facilitates semiautomated retrospective valve tracking, using two orthogonal cine MRI acquisitions to locate the valve annulus during each cardiac phase. As a result, the quantification plane closely follows the valve orifice throughout the cardiac cycle. This is especially valuable for the atrio-ventricular heart valves, which have a complex valvular and annular anatomy and are highly dynamic. The use of 2D PC-MRI to measure net flows over the mitral valve (MV) and tricuspid valve (TV) has been associated with markedly lower correlations between valves than 4D flow MRI with valve tracking (Pearson's  $r = 0.34$ ,  $P = 0.34$  for 2D PC-MRI as opposed to  $r = 0.91$ ,  $P < 0.01$  for 4D flow MRI).<sup>23</sup>

Furthermore, various advanced hemodynamic parameters can be extracted from 4D flow MRI-acquired data. In this section we provide a brief overview of 4D flow MRI-derived hemodynamic parameters that may aid in the clinical evaluation of left-sided VHD. The application of 4D flow MRI to AS, AR, and MVR as proposed in the current literature will be discussed in the subsequent section.

### Wall Shear Stress

Wall shear stress (WSS) is defined as the viscous shear force of flowing blood acting tangentially on the vessel wall. It is the frictional force of the blood on the vascular endothelium and has been associated with vessel wall remodeling.<sup>24</sup> 4D flow MRI can be used to calculate regional aortic WSS from near-wall blood flow velocity gradients.<sup>25</sup> Figure 2 shows examples of peak systolic patient-specific velocity vectors and cohort-averaged WSS patterns in the thoracic aorta of patients with aortic dilatation distal to a trileaflet aortic valve with and without AS. Histological validation shows that regions with increased WSS are subject to extracellular matrix degradation and elastic fiber degeneration in the ascending aorta of patients with bicuspid aortic valve (BAV) disease.<sup>26</sup> Longitudinal studies will have to determine whether WSS is a good predictor of aortopathy in patients with aortic valve disease.

### Flow Displacement

Flow displacement is a parameter used to quantify the eccentricity of the flow jet in the ascending aorta. It is defined as the distance between the velocity-weighted center of the peak systolic flow jet and the ascending aorta luminal centerline (Fig. 3). High degrees of flow displacement have been observed in patients with AS, BAV disease, and after transcatheter aortic valve replacement (TAVR).<sup>27–30</sup> A study in 25 BAV patients has shown that typical displacements differ between various BAV morphologies and correspond with patterns of dilative aortopathy.<sup>31</sup> Moreover, flow displacement correlated with the aortic growth rate, making this parameter a potential risk marker in patients susceptible to valve-induced aortic dilatation.

### Flow Component Analysis

Flow component analysis using particle tracing can provide insight into the efficiency of the cardiac cycle. Blood transiting the LV may follow different paths that can be specified by spatial origin and destination over the cardiac cycle, allowing for the definition of four components: 1) direct flow, ie,

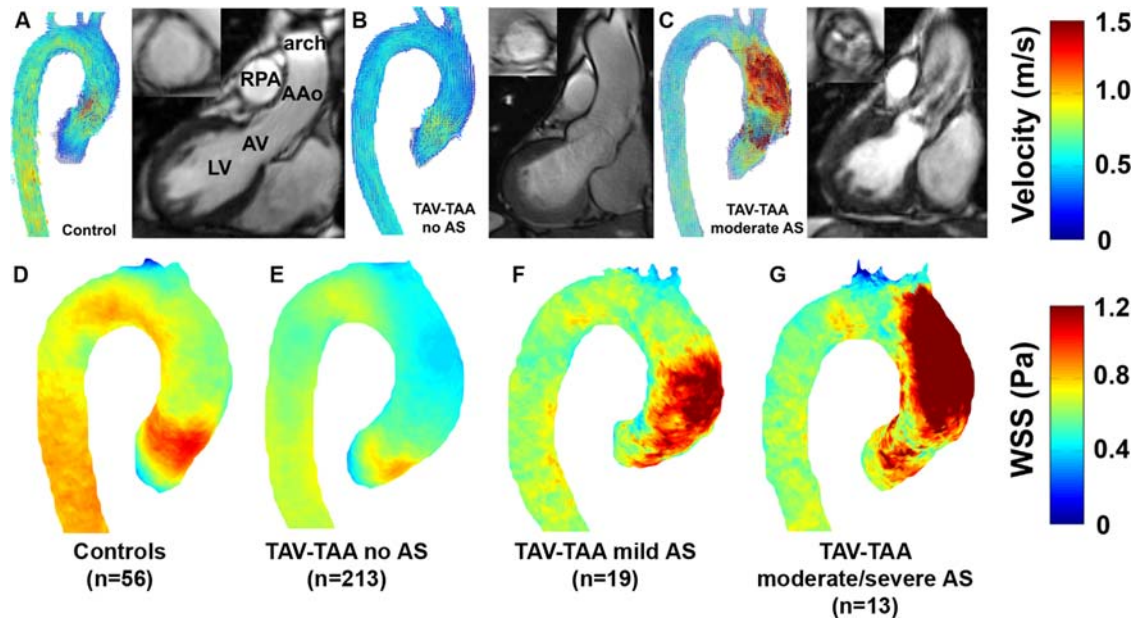


**FIGURE 2:** Exemplary 3D velocity vector visualizations and bSSFP images of the trileaflet valve and the left ventricular outflow tract in (A) a healthy control showing full opening of the valve, (B) a patient with a trileaflet aortic valve (TAV) and a thoracic aortic aneurysm (TAA)—velocities are lower than in the control—and (C) a patient with a stenosed trileaflet aortic valve showing high velocities. LV, left ventricle; AV, aortic valve; AAO, ascending aorta; RPA, right pulmonary artery. (D–G) Cohort-averaging of WSS shows that WSS is lower for patients with TAV-TAA without AS, whereas WSS increases when AS severity increases. (Adapted from: van Ooij P, Markl M, Collins JD, et al. Aortic valve stenosis alters expression of regional aortic wall shear stress: New insights from a 4-dimensional flow magnetic resonance imaging study of 571 subjects. *J Am Heart Assoc* 2017;6:e005959; Available from, DOI: 10.1161/JAHA.117.005959, with permission.)

blood entering and leaving the LV in the same cardiac cycle; 2) retained flow, ie, blood that enters the LV but is not ejected during systole; 3) delayed ejected flow, ie, blood that already resides in the LV before diastole and is ejected during subsequent systole; and 4) residual volume, ie, blood that already resides in the LV before diastole and stays there during systole (Fig. 4).<sup>32</sup> These components can in turn be analyzed based on kinetic energy (KE). Flow component analysis (together with KE analysis) may in particular prove useful for the evaluation of complicated VHD phenotypes like low-flow low-gradient AS or combined VHD, as current clinical parameters do not always suffice in determining the severity and origin of these diseases.<sup>33</sup>

### Vortical Flow Patterns

Passage of blood across the heart valves leads to a certain degree of flow disturbance, depending on valvular function. As a result, KE is converted into thermal energy in a process called viscous energy loss.<sup>34</sup> Formation of vortices downstream of the heart valves minimizes this energy loss.<sup>35</sup> Visual and quantitative evaluation of vortical flow by 4D flow MRI is particularly relevant for the assessment of diastolic LV inflow.<sup>36</sup> Vortex formation during LV inflow is a natural phenomenon that is believed to be important for redirection of blood towards the LV outflow tract, and thus for efficient cardiac function.<sup>37</sup> A recent 4D flow MRI study in 32 patients who underwent atrioventricular septal defect (AVSD) repair revealed significant differences in vortex presence, position,

shape, and orientation compared to healthy subjects (see Fig. 5).<sup>38</sup> Furthermore, vortex core shape and orientation were strongly related to valve shape and LV inflow direction.

### Turbulent Kinetic Energy

Whereas viscous energy loss is related to flow inefficiency in nonturbulent flow such as vortical and helical flow, turbulent kinetic energy (TKE) reflects flow inefficiency in regions of flow disturbance characterized by rapid velocity fluctuations in different directions, often referred to as turbulence.<sup>39,40</sup> 4D flow MRI can be used to derive velocity distributions in individual voxels and subsequently calculate TKE and pressure gradients. As heat dissipation is not accounted for in TKE calculations based on three-directional 4D flow MRI, Ha et al proposed the use of a six-directional 4D flow encoding scheme to quantify TKE.<sup>41</sup> They show that this method can robustly predict the irreversible pressure drop in a phantom stenosis model.<sup>41</sup>

## Application of 4D Flow MRI to Left-Sided VHD

### Aortic Valve Stenosis

Severe AS can lead to symptoms such as dyspnea, angina, and syncope and is a major cause of morbidity and mortality worldwide.<sup>1</sup> Grading of AS severity by MRI is typically based on peak blood flow velocity or AVA assessment using 2D PC-MRI, to estimate the transvalvular pressure gradient, and/or AVA.<sup>1,42</sup> Echocardiographic estimation of pressure



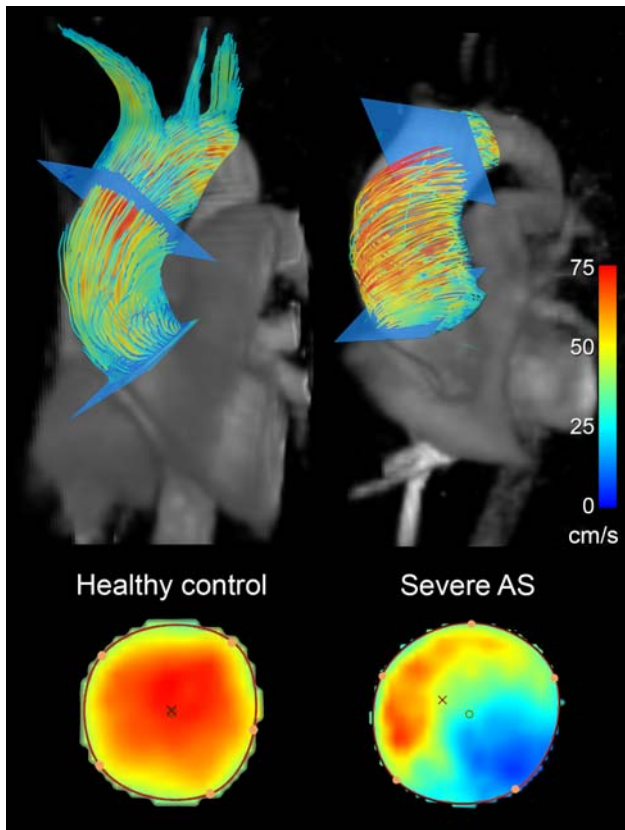


**FIGURE 3:** Differences in blood flow eccentricity between a 26-year-old healthy control (left) and a 21-year-old patient with severe AS accepted for surgical aortic valve replacement (right). Pathlines (top) show a more helical flow pattern for the AS patient than for the healthy control. Cross-sectional views of the velocities in the mid-ascending aorta (bottom) give insight into the flow displacement, which is defined by the distance between the center of the blood flow (indicated by the cross) and the centerline of the vessel (indicated by the circle) and is normalized to the lumen diameter.

gradients has demonstrated systematic discrepancies between Doppler-based and catheter-based measurements.<sup>43</sup> These discrepancies were assigned to pressure loss overestimation by Doppler echocardiography due to the pressure recovery phenomenon downstream of the aortic valve, and consequently overestimation of AS severity. 4D flow-derived estimation of transvalvular pressure gradients based on TKE has been proposed as a supplementary method in the evaluation of AS,<sup>44,45</sup> as it allows for functional analysis of energy efficiency and cardiac workload that echocardiography does not offer. The clinical value of 4D flow-derived TKE is supported by good correlations between TKE values in the ascending aorta and poststenotic pressure loss in AS patients.<sup>32,46</sup> Furthermore, in AS patients with aortic dilatation, elevated 4D flow-derived viscous energy loss in both the ascending and thoracic aorta strongly correlated with the transvalvular pressure gradient as calculated with the modified Bernoulli equation.<sup>47,48</sup> Another 4D flow study has focused on quantification of the effective orifice area (EOA) to determine AS severity, employing a method called jet shear layer detection.<sup>49</sup> This method uses a mathematical approach to distinguish flow jets from recirculating flow to reveal a "shear layer" that represents the EOA border at the height of the vena contracta.

4D flow MRI may also aid in the assessment of VHD-induced aortic dilatation. Several 4D flow MRI studies show that the presence and severity of AS determine the extent of abnormal hemodynamics throughout the entire ascending aorta, giving rise to elevated WSS and subsequent extracellular matrix degradation and elastic fiber degeneration in the ascending aorta.<sup>26,50,51</sup>

Treatment of severe AS consists of replacement of the stenotic valve through surgical aortic valve replacement (SAVR) or, predominantly in elderly or high-risk patients, transcatheter aortic valve replacement (TAVR).<sup>42</sup> Technical

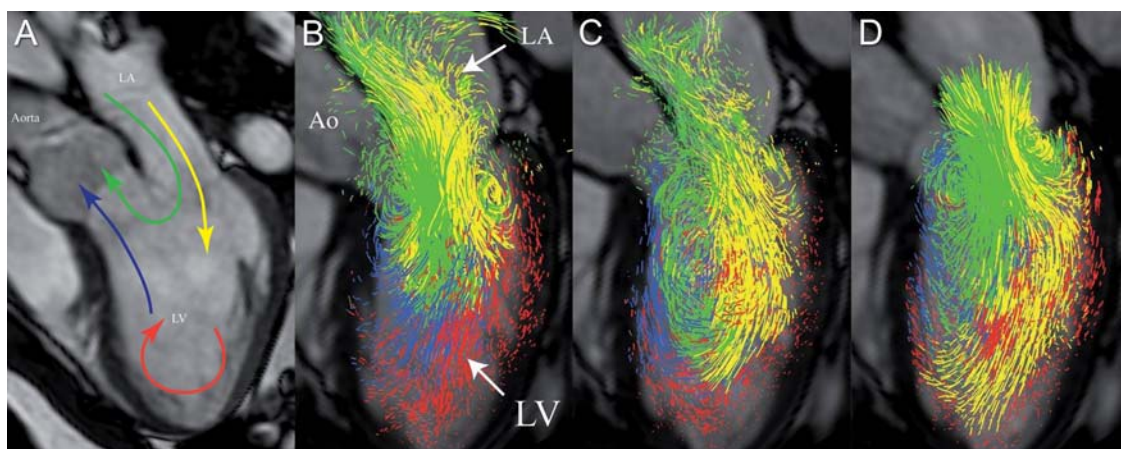


**FIGURE 4:** (A) Illustration of the four functional components of LV blood flow: direct flow, green; retained flow, yellow; delayed ejected flow, blue; residual volume, red. (B–D) Pathline visualizations of the four components in a healthy 50-year-old woman during (B) early diastole, (C) diastasis, and (D) atrial contraction. Ao, aorta; LV, left ventricle; LA, left atrium. (Adapted from: Eriksson J, Bolger AF, Ebbers T, Carlhäll CJ. Four-dimensional blood flow-specific markers of LV dysfunction in dilated cardiomyopathy. *Eur Heart J Cardiovasc Imaging* 2013;14:417–424, by permission of Oxford University Press on behalf of the European Society of Cardiology.)

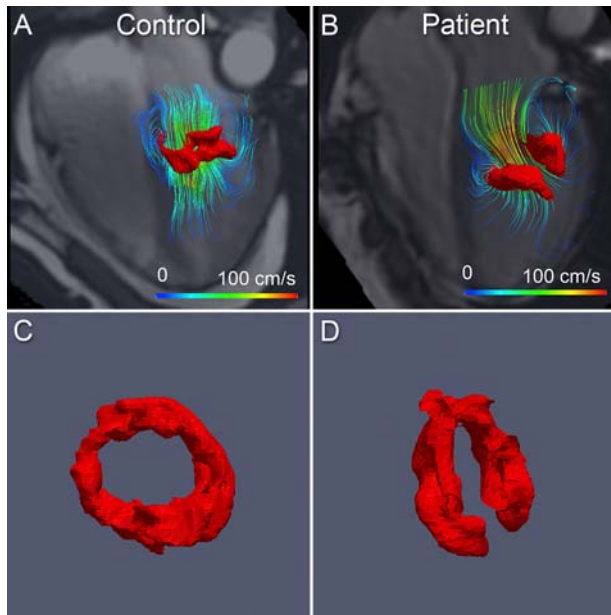


**FIGURE 5:** Different vortex core orientation and shape during early diastole in a patient with corrected atrioventricular septal defect (AVSD) (B,D) compared with a healthy control (A,C). Streamline visualizations show a more lateral inflow direction in the patient (B) compared to the healthy control (A). LA, left atrium; LV, left ventricle. (Adapted from: Calkoen EE, Westenberg JJ, Kroft LJ, et al. Characterization and quantification of dynamic eccentric regurgitation of the left atrioventricular valve after atrioventricular septal defect correction with 4D Flow cardiovascular magnetic resonance and retrospective valve tracking. *J Cardiovasc Magn Reson* 2012;17:1–9, with permission.)

developments in both image acquisition and prosthetic valve designs have made MRI in patients with aortic valve prostheses possible, allowing for the evaluation of blood flow characteristics after AVR. 4D flow MRI studies focusing on the hemodynamic performance of prosthetic aortic valves have compared various biological aortic valves, mechanical aortic valves, and transcatheter aortic valve implants.<sup>52,53</sup> These studies show that after AVR, ascending aortic hemodynamics are different compared to native aortic valves and that blood flow velocities and WSS vary between different types of prostheses. Future 4D flow MRI studies are necessary to determine whether these differences between prostheses, such as differences in WSS patterns, have a prognostic value and may aid in patient-specific treatment selection.

### Aortic Valve Regurgitation

AR is most often caused by BAV, infective endocarditis, or dilatation of the aortic root caused by connective tissue disease.<sup>1</sup> Quantitative MRI assessment of AR consists of LV volume assessment and aortic flow measurements. Treatment may consist of surgical aortic valve replacement, aortic valve repair, or valve-sparing aortic root replacement. Timing of treatment is based on several factors, including LV ejection fraction (LVEF), LV diameters, and the presence of symptoms. Several small studies have shown that MRI-derived

regurgitant volume may provide important prognostic information in AR patients<sup>54–56</sup> and supersedes TTE-derived regurgitant volume in its association with outcome.<sup>54</sup>

Research on the role of 4D flow MRI in patients with AR is limited. A study of 54 patients showed that visual, qualitative grading of AR is well possible with 4D flow MRI in patients with mild to moderate AR and leads to good agreement with TTE-based severity grading ( $\kappa = 0.73$ ).<sup>57</sup> 4D flow MRI with valve tracking has been used as a reference method for quantification of AR with 2D and 3D Doppler echocardiography. 2D Doppler echocardiography showed a moderate agreement with 4D flow MRI in qualitative severity grading ( $\kappa = 0.53$ ), in part due to eccentric jets which were associated with weak correlation with 4D flow MRI-based quantification ( $r = 0.66$ ,  $P = 0.005$ ).<sup>58</sup> These results suggest that, especially for eccentric jets and noncircular valve orifices, 4D flow MRI and 3D TTE can capture regurgitation better than 2D TTE because they are not limited by geometrical assumptions and suboptimal alignment with the flow jet. Furthermore, 4D flow MRI studies using valve tracking in a study population of healthy subjects as well as AR patients demonstrated strong consistency between net flow volumes across all four heart valves.<sup>21,22</sup>

### Mitral Valve Regurgitation

MVR is the most prevalent form of left-sided VHD. It can cause LV volume overload, which may lead to progressive dilatation of the left ventricle and left atrium, heart failure, and pulmonary hypertension.<sup>6</sup> Decisions regarding surgical interventions, being mitral valve repair or replacement, rely on symptomatology as well as the regurgitation severity, LVEF, and LV end-systolic diameter.

MRI has been proposed as an accurate and reproducible method for the quantification of MVR and has been associated with more reproducible severity grading than echocardiography.<sup>59–61</sup> Since direct 2D phase-contrast (PC) MRI over the mitral valve does not optimally account for annular motion and the valve's complex anatomy, quantification of regurgitant volume is typically performed in an indirect manner based on LV stroke volume and aortic flow.<sup>62</sup> A large multicenter study revealed a considerable discordance in categorical severity grading between MRI and echocardiography.<sup>61</sup> Interestingly, in a subgroup of patients undergoing mitral valve surgery, MRI-based severity grading had superior prognostic value over echocardiography in predicting the degree of postsurgical LV remodeling. Also, recent large-scale studies found MRI-derived regurgitant volume to be a better predictor of referral for surgery and all-cause mortality than echocardiographic parameters.<sup>63,64</sup> These findings may evoke changes in the diagnostic and prognostic workup of MVR patients, causing MRI to gain ground in the clinical management of these patients.

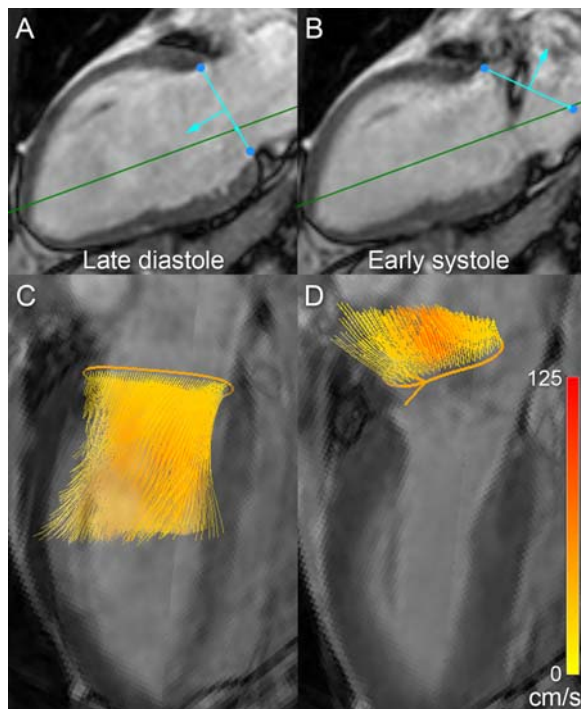


**FIGURE 6:** Retrospective valve tracking procedure on 4D flow MRI data in a patient with asymptomatic severe MVR, as first diagnosed by echocardiography. (A) The mitral valve is tracked on a two-chamber and four-chamber cine bSSFP image (green line shows the location of intersection). (B) The quantification plane is angulated perpendicular to the regurgitation and shifted upward towards the vena contracta to minimize phase dispersion effects close to the valve. Corresponding time-resolved streamlines are shown in (C,D). A regurgitation fraction of 44% was measured.

4D flow MRI in combination with retrospective valve tracking enables accurate transmitral flow quantification. An early study demonstrated excellent correlation between net forward MV and tricuspid valve (TV) flow volumes ( $r = 0.97$ ,  $P < 0.01$ ) and good correlation with aortic valve (AV) forward flow ( $r = 0.82$ ,  $P < 0.01$  and  $r = 0.74$ ,  $P < 0.01$  for MV and TV, respectively) in 20 patients suspected of having mitral and/or tricuspid valve regurgitation.<sup>23</sup> Excellent consistency between mitral and aortic valve flow ( $r = 0.97$ ,  $P < 0.001$ ) has been obtained even for complex regurgitant flow jets in MVR patients who underwent AVSD correction.<sup>19</sup> See Fig. 6 for an example of valve tracking in a patient with severe MVR. Also, MVR patients with eccentric regurgitation jets have demonstrated highly disturbed left atrial flow patterns with elevated left atrial TKE levels, which were, averaged over the cardiac cycle, closely related to net regurgitant volumes.<sup>65</sup> Further characterization of left atrial flow in MVR patients could render new insights into both accurate quantification of MVR and the mechanisms driving disease progression.

Retrospective studies with 4D flow MRI on surgical cohorts increasingly demonstrate the prognostic value of hemodynamic parameters. Al-Wakeel et al studied the effect of MV repair on KE in patients with MVR and found that

MV repair resulted in normalization of systolic and early diastolic KE values, mainly due to reductions of blood volumes.<sup>66</sup> The effect of MV repair on normal LV hemodynamics has been assessed with 4D flow MRI as well, using mitral annuloplasty rings of different sizes implanted in healthy sheep.<sup>67</sup> Intraventricular flow patterns were shown to be disturbed after annuloplasty, with a significant relation between the size of the annuloplasty ring and the inflow angle, as well as peak-diastolic velocity.

## Tissue Characterization and Myocardial Function Assessment by Advanced MRI Techniques

### Tissue Mapping

In patients with left-sided VHD, LV remodeling is an important marker of disease progression. It is often characterized by progressive myocardial fibrosis, resulting in LV systolic dysfunction.<sup>68</sup> Tissue mapping is a novel MRI modality, capable of visualizing and quantifying structural changes in the myocardium. Images are based on the MRI characteristics  $T_1$ ,  $T_2$ , and  $T_2^*$  (star) of the myocardium and allow for quantification of both intracellular abnormalities (such as cytogenic edema and iron overload), extracellular abnormalities (such as vasogenic edema and fibrosis), or a combination of both.<sup>69</sup>

### $T_1$ -Mapping and Extracellular Volume Calculation

$T_1$  values are a marker for myocardial fibrosis or tissue inflammation: important markers of disease progression in patients with left-sided VHD. In AS patients, mechanisms leading to myocardial fibrosis include diffuse ischemia in hypertrophic LV myocardium as a consequence of chronic pressure overload.<sup>70,71</sup> In AR and MVR, volume overload causes activation of the renin-angiotensin-aldosterone system, which activates profibrotic pathways in the myocardium.<sup>72,73</sup> Myocardial fibrosis can be quantified through myocardial biopsy, but recent studies have shown that extracellular volume (ECV), a proxy of diffuse myocardial fibrosis, can be quantified using  $T_1$ -mapping. This technique allows for measurement of native  $T_1$  values of the myocardium and gadolinium-enhanced  $T_1$ -shortening; parameters that, after correction for hematocrit levels, can be used to quantify the amount of ECV in the myocardial volume of interest. Various protocols have been proposed for the acquisition of  $T_1$ -maps, such as the modified Look-Locker inversion recovery (MOLLI) technique as described by Messroghli et al.<sup>74</sup> Although ECV mapping is traditionally performed using slow intravenous gadolinium infusion, several studies have shown that both simple bolus contrast administration and split dose contrast administration allow for myocardial ECV fraction measurements.<sup>75-77</sup> These developments may accelerate the introduction of ECV mapping into routine clinical MRI protocols.



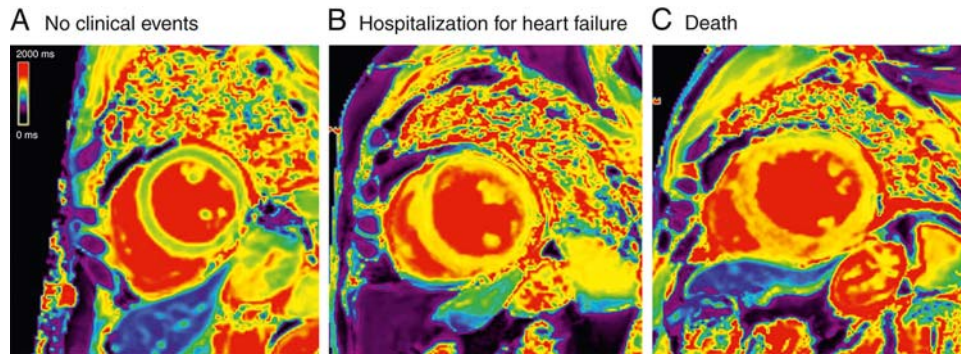


**FIGURE 7:** Color-coded native T<sub>1</sub>-weighted images of a mid-ventricular LV slice of (A) a 63-year-old man with moderate AS who did not experience any clinical event, (B) a 70-year-old man with severe AS who was hospitalized for decompensated heart failure, and (C) a 65-year-old man with severe AS who died during follow-up. Native T<sub>1</sub>-values as measured in a septal region of interest were 1,163 msec, 1,257 msec, and 1,358 msec, respectively. (Adapted from: Lee H, Park J-B, Yoon YE, et al. Noncontrast myocardial T<sub>1</sub> mapping by cardiac magnetic resonance predicts outcome in patients with aortic stenosis. *JACC Cardiovasc Imaging* 2017;1-10, with permission from Elsevier.)

Wong et al found, in an unselected cohort of patients undergoing cardiac MRI, that ECV is a strong predictor of mortality.<sup>78</sup> Several studies in AS patients have shown that T<sub>1</sub> values and the degree of myocardial fibrosis correlate with disease progression and mortality and that myocardial ECV is a strong predictor of cardiovascular complications<sup>70,71,79-81</sup> (Fig. 7). Moreover, recent studies in AS patients indicate that T<sub>1</sub>-mapping may aid in the detection of cardiac amyloidosis, which can significantly influence the prognosis.<sup>82</sup> Hence, T<sub>1</sub>-mapping can be useful in the diagnostic work-up and the prognostic evaluation of AS patients.<sup>82-85</sup>

In AR patients, T<sub>1</sub>-mapping has revealed differences in myocardial relaxation times compared to normal hearts.<sup>86</sup> Furthermore, increased ECV and diffuse fibrosis were found in patients with asymptomatic moderate to severe MVR.<sup>86-89</sup> Future T<sub>1</sub>- and ECV-mapping studies are required to investigate whether the finding of myocardial fibrosis in patients with left-sided VHD mandates early surgical intervention to prevent progressive and irreversible myocardial fibrosis. Interestingly, early studies in patients with BAV and hypertrophic cardiomyopathy show that the combination of 4D flow MRI with tissue mapping allows for comprehensive evaluation of flow and tissue abnormalities that may lead to LV remodeling.<sup>90,91</sup>

### Strain Imaging

Strain imaging allows for dynamic assessment of LV function, reflecting the contractility of the myocardial wall. With MRI, strain can be measured longitudinally, circumferentially, and radially using long-axis and short-axis cine images, typically by means of feature tracking over 16 myocardial segments as defined by the American Heart Association (AHA) model. An example is shown in Fig. 8. This approach provides a simplified model of myocardial motion based on tracking of the myocardial borders and allows for quantification of global strain and strain rate, surrogates for diastolic function. In a large meta-analysis, global longitudinal strain (GLS), as assessed by echocardiography, has shown to be more

predictive of mortality than LVEF in patients with LV dysfunction.<sup>92</sup> The potential of GLS has also been investigated specifically in VHD patients. A study comprising 233 patients with severe MVR undergoing mitral valve repair identified impaired GLS as an independent predictor of LV dysfunction (LVEF <50%) during long-term follow-up.<sup>93</sup> These patients had a normal EF at the time of surgery and still developed LV dysfunction postoperatively, indicating that myocardial damage as a consequence of MVR may occur before LV function deteriorates. Indeed, in a cohort of asymptomatic MVR patients ( $n = 737$ ) with preserved LVEF, abnormal baseline GLS was independently associated with long-term mortality.<sup>94</sup> Moreover, impaired longitudinal and circumferential strain rates 6 months after MV repair have been associated with myofibrillar degeneration at the time of surgery,<sup>95,96</sup> signifying the clinical value of impaired strain as an imaging biomarker of early myocardial dysfunction. Also for AR, long-term studies show that GLS is an independent predictor of mortality or indications for surgery.<sup>97-99</sup> Outcome studies with similar results have been conducted in AS patients.<sup>100-102</sup>

Hence, future adoption of GLS evaluation into standard clinical practice may lead to improved surgical timing in patients with VHD. However, the application of strain imaging for the assessment of LV function has so far not explicitly appeared in guidelines for the clinical management of VHD. Although most aforementioned strain studies employed echocardiographic methods, a recent comparison of echocardiographic speckle tracking with MRI-based feature tracking showed that MRI is a useful alternative to echocardiography for global strain analysis and more practicable due to better image quality.<sup>103</sup>

### Future Perspectives and Conclusion

This review demonstrates the potential of 4D flow MRI, tissue mapping, and strain imaging for the diagnosis and quantitative assessment of left-sided VHD. Longitudinal studies on



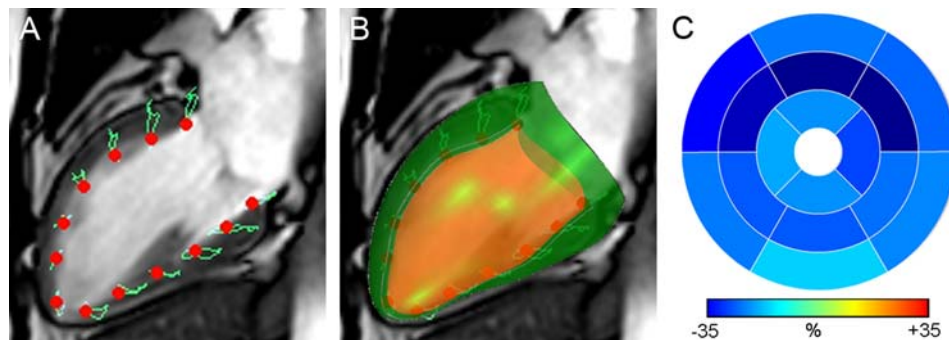


**FIGURE 8:** Longitudinal strain analysis of the left ventricle using feature tracking. Cardiac MRI images were obtained in a 59-year-old healthy person. **(A)** Two-chamber cine bSSFP image with tracked points in red and time-resolved trajectories in green. **(B)** Superimposed 3D model showing end-systolic (orange) and end-diastolic LV volume (green), obtained by combining feature tracking analyses in two-chamber, three-chamber, and four-chamber view. **(C)** AHA 16-segment model of longitudinal strain percentages.

the natural course of AS, AR, and MVR as well as large-scale outcome studies on surgical patients are of great importance to prospectively investigate the relation between disease development and MRI-derived hemodynamic and tissue-characteristic parameters. Furthermore, research is ongoing to overcome various limitations. In 4D flow MRI, perhaps the largest challenge is to keep scan times low while reaching higher spatiotemporal resolutions in large volumes of interest. Also, postprocessing is time-consuming and user- and experience-dependent, delaying the implementation of these techniques into general clinical practice. Technical developments, such as acceleration of acquisition sequences using parallel imaging or k-t undersampling, may allow for more efficient data acquisition and analysis. To date, only a few commercial 4D flow MRI sequences and packages have been introduced to the market, and most 4D flow studies and applications rely on protocols developed by individual research groups. The wide variety of used sequences and analysis software forms an obstacle for the development of 4D flow MRI to become a commonly employed clinical technique.

In tissue mapping, imaging studies have mainly been conducted in small cohorts and the accuracy of  $T_1$  values remains unclear. Although consensus-based recommendations for parametric mapping exist, histopathological validation of  $T_1$ -mapping studies will have to clarify whether tissue mapping can be used for diagnostic and prognostic purposes.<sup>69</sup> Strain imaging has not been performed as widely with MRI as with echocardiography, although it is feasible on routine MRI images and its prognostic value is supported by a large body of echocardiographic studies. Intervendor differences, however, might hamper the clinical implementation of strain imaging.<sup>104</sup>

In conclusion, advanced cardiac MRI techniques provide valuable information that may guide clinical decision-making and surgical planning in patients with left-sided VHD. Future research should aim at exploring quantitative MRI to its full potential in the optimization and fine-tuning

of clinical management in VHD. Employment of quantitative 4D flow MRI, multiparametric mapping, and strain quantification in combination with standard quantitative volumetry and qualitative imaging (such as contrast-enhanced MRA) ushers in a new era of increasingly accurate diagnosis, risk stratification, treatment selection, and planning for best patient outcome.

### Conflict of Interest

The authors report no conflicts of interest.

### References

1. Baumgartner H, Falk V, Bax JJ, et al. 2017 ESC/EACTS Guidelines for the management of valvular heart disease. *Eur Heart J* 2017;38:2739–2786.
2. Chambers JB, Myerson SG, Rajani R, Morgan-Hughes GJ, Dweck MR. Multimodality imaging in heart valve disease. *Open Heart* 2016;3:e000330.
3. Myerson SG. Heart valve disease: investigation by cardiovascular magnetic resonance. *J Cardiovasc Magn Reson* 2012;14:7.
4. Nkomo VT, Gardin JM, Skelton TN, Gottdiener JS, Scott CG, Enriquez-Sarano M. Burden of valvular heart diseases: a population-based study. *Lancet* 2006;368:1005–1011.
5. Wollersheim LW, Li WW, De Mol BA. Current status of surgical treatment for aortic valve stenosis. *J Card Surg* 2014;29:630–637.
6. Levine RA, Hagège AA, Judge DP, et al. Mitral valve disease-morphology and mechanisms. *Nat Rev Cardiol* 2015;12:689–710.
7. Grothues F, Smith GC, Moon JC, et al. Comparison of interstudy reproducibility of cardiovascular magnetic resonance with two-dimensional echocardiography in normal subjects and in patients with heart failure or left ventricular hypertrophy. *Am J Cardiol* 2002;90:29–34.
8. Allen BD, Syed AA, Bollache E, et al. Cardiovascular MRI in thoracic aortopathy: a focused review of recent literature updates. *Curr Radiol Rep* 2017 Oct;5:50.
9. Chitiboi T, Axel L. Magnetic resonance imaging of myocardial strain: A review of current approaches. *J Magn Reson Imaging* 2017;46:1263–1280.
10. Zamorano JL, Fernández-Golfín C, González-Gómez A. Quantification of mitral regurgitation by echocardiography. *Heart* 2015;101:146–154.

11. Chen C, Thomas JD, Anconina J, et al. Impact of impinging wall jet on color Doppler quantification of mitral regurgitation. *Circulation* 1991;84:712–720.
12. Sugeng L, Spencer KT, Mor-Avi V, et al. Dynamic three-dimensional color flow Doppler: An improved technique for the assessment of mitral regurgitation. *Echocardiography* 2003;20:265–273.
13. Thavendiranathan P, Phelan D, Thomas JD, Flamm SD, Marwick TH. Quantitative assessment of mitral regurgitation: Validation of new methods. *J Am Coll Cardiol* 2012;60:1470–1483.
14. Zoghbi WA, Adams D, Bonow RO, et al. Recommendations for noninvasive evaluation of native valvular regurgitation: a report from the American Society of Echocardiography developed in collaboration with the Society for Cardiovascular Magnetic Resonance. *J Am Soc Echocardiogr* 2017;30:303–371.
15. Elliott PM, Anastasakis A, Borger MA, et al. 2014 ESC Guidelines on diagnosis and management of hypertrophic cardiomyopathy. *Eur Heart J* 2014;35:2733–2779.
16. Bellenger N, Burgess MI, Ray SG, et al. Comparison of left ventricular ejection fraction and volumes in heart failure by echocardiography, radionuclide ventriculography and cardiovascular magnetic resonance. Are they interchangeable? *Eur Heart J* 2000;21:1387–1396.
17. Dyverfeldt P, Bissell M, Barker AJ, et al. 4D flow cardiovascular magnetic resonance consensus statement. *J Cardiovasc Magn Reson* 2015;17:1–19.
18. Nordmeyer S, Riesenkampff E, Messroghli D, et al. Four-dimensional velocity-encoded magnetic resonance imaging improves blood flow quantification in patients with complex accelerated flow. *J Magn Reson Imaging* 2013;37:208–216.
19. Calkoen EE, Westenberg JJ, Kroft LJ, et al. Characterization and quantification of dynamic eccentric regurgitation of the left atrioventricular valve after atrioventricular septal defect correction with 4D flow cardiovascular magnetic resonance and retrospective valve tracking. *J Cardiovasc Magn Reson* 2012;17:1–9.
20. Rose MJ, Jarvis K, Chowdhary V, et al. Efficient method for volumetric assessment of peak blood flow velocity using 4D flow MRI. *J Magn Reson Imaging* 2016;44:1673–1682.
21. Roes SD, Hammer S, van der Geest RJ, et al. Flow assessment through four heart valves simultaneously using 3-dimensional 3-directional velocity-encoded magnetic resonance imaging with retrospective valve tracking in healthy volunteers and patients with valvular regurgitation. *Invest Radiol* 2009;44:669–675.
22. Hsiao A, Tariq U, Alley MT, Lustig M, Vasanawala SS. Inlet and outlet valve flow and regurgitant volume may be directly and reliably quantified with accelerated, volumetric phase-contrast MRI. *J Magn Reson Imaging* 2015;41:376–385.
23. Westenberg JJ, Roes SD, Ajmone Marsan N, et al. Mitral valve and tricuspid valve blood flow: accurate quantification with 3D velocity-encoded MR imaging with retrospective valve tracking. *Radiology*. 2008;249:792–800.
24. Lehoux S, Tedgui A. Cellular mechanics and gene expression in blood vessels. *J Biomech* 2003;36:631–643.
25. van Ooij P, Potters WW, Collins J, et al. Characterization of abnormal wall shear stress using 4D flow MRI in human bicuspid aortopathy. *Ann Biomed Eng* 2015;43:1385–1397.
26. Guzzardi DG, Barker AJ, Van Ooij P, et al. Valve-related hemodynamics mediate human bicuspid aortopathy: insights from wall shear stress mapping. *J Am Coll Cardiol* 2015;66:892–900.
27. Sigovan M, Hope MD, Dyverfeldt P, Saloner D. Comparison of four-dimensional flow parameters for quantification of flow eccentricity in the ascending aorta. *J Magn Reson Imaging* 2011;34:1226–1230.
28. Bissell MM, Hess AT, Biasioli L, et al. Aortic dilation in bicuspid aortic valve disease: flow pattern is a major contributor and differs with valve fusion type. *Circ Cardiovasc Imaging* 2013;6:499–507.
29. Hope MD, Dyverfeldt P, Acevedo-Bolton G, et al. Post-stenotic dilation: Evaluation of ascending aortic dilation with 4D flow MR imaging. *Int J Cardiol* 2012;156:e40–42.
30. Markl M, Mikati I, Carr J, McCarthy P, Malaisrie SC. Three-dimensional blood flow alterations after transcatheter aortic valve implantation. *Circulation* 2012;125:e573–575.
31. Hope MD, Sigovan M, Wrenn SJ, Saloner D, Dyverfeldt P. MRI hemodynamic markers of progressive bicuspid aortic valve-related aortic disease. *J Magn Reson Imaging* 2014;40:140–145.
32. Eriksson J, Carlhäll C, Dyverfeldt P, Engvall J, Bolger AF, Ebbers T. Semi-automatic quantification of 4D left ventricular blood flow. *J Cardiovasc Magn Reson* 2010;12:9.
33. Pibarot P, Dumesnil JG. Low-flow, low-gradient aortic stenosis with normal and depressed left ventricular ejection fraction. *J Am Coll Cardiol* 2012;60:1845–1853.
34. Akins CW, Travis B, Yoganathan AP. Energy loss for evaluating heart valve performance. *J Thorac Cardiovasc Surg* 2008;136:820–833.
35. Pedrizzetti G, Domenichini F. Nature optimizes the swirling flow in the human left ventricle. *Phys Rev Lett* 2005;95:1–4.
36. Töger J, Kanski M, Carlsson M, et al. Vortex Ring Formation in the Left Ventricle of the Heart: Analysis by 4D Flow MRI and Lagrangian Coherent Structures. *Ann Biomed Eng* 2012;40:2652–2662.
37. Kilner PJ, Yang G-Z, John Wilkes A, Mohiaddin RH, Firmin DN, Yacoub MH. Asymmetric redirection of flow through the heart. *Nature* 2000;404:759–761.
38. Calkoen EE, Elbaz MSM, Westenberg JJM, et al. Altered left ventricular vortex ring formation by 4-dimensional flow magnetic resonance imaging after repair of atrioventricular septal defects. *J Thorac Cardiovasc Surg* 2015;150:1233–1240.
39. Dyverfeldt P, Sigfridsson A, Kvitting JPE, Ebbers T. Quantification of intravoxel velocity standard deviation and turbulence intensity by generalizing phase-contrast MRI. *Magn Reson Med* 2006;56:850–858.
40. Dyverfeldt P, Kvitting JPE, Sigfridsson A, Engvall J, Bolger AF, Ebbers T. Assessment of fluctuating velocities in disturbed cardiovascular blood flow: In vivo feasibility of generalized phase-contrast MRI. *J Magn Reson Imaging* 2008;28:655–663.
41. Ha H, Lantz J, Ziegler M, et al. Estimating the irreversible pressure drop across a stenosis by quantifying turbulence production using 4D flow MRI. *Sci Rep* 2017;7:46618.
42. Nishimura RA, Otto CM, Bonow RO, et al. 2014 AHA/ACC guideline for the management of patients with valvular heart disease: A report of the American College of Cardiology/American Heart Association task force on practice guidelines. *J Am Coll Cardiol* 2014;63:2438–2488.
43. Garcia D, Dumesnil JG, Durand LG, Kadem L, Pibarot P. Discrepancies between catheter and doppler estimates of valve effective orifice area can be predicted from the pressure recovery phenomenon: Practical implications with regard to quantification of aortic stenosis severity. *J Am Coll Cardiol* 2003;41:435–342.
44. Binter C, Gotschy A, Sündermann SH, et al. Turbulent kinetic energy assessed by multipoint 4-dimensional flow magnetic resonance imaging provides additional information relative to echocardiography for the determination of aortic stenosis severity. *Circ Cardiovasc Imaging*. 2017;10(6).
45. Ha H, Kim GB, Kweon J, et al. Turbulent kinetic energy measurement using phase contrast MRI for estimating the poststenotic pressure drop: In vitro validation and clinical application. *PLoS One* 2016;11:1–14.
46. Dyverfeldt P, Hope MD, Tseng EE, Saloner D. Magnetic resonance measurement of turbulent kinetic energy for the estimation of irreversible pressure loss in aortic stenosis. *JACC Cardiovasc Imaging* 2013;6:64–71.
47. Barker AJ, van Ooij P, Bandi K, et al. Viscous energy loss in the presence of abnormal aortic flow. *Magn Reson Med* 2014;72:620–628.
48. Garcia D, Pibarot P, Dumesnil JG, Sakr F, Durand L-G. Assessment of aortic valve stenosis severity?: A new index based on the energy loss concept. *Circulation* 2000;101:765–771.
49. Garcia J, Markl M, Schnell S, et al. Evaluation of aortic stenosis severity using 4D flow jet shear layer detection for the measurement of valve effective orifice area. *Magn Reson Imaging*. 2014;32:891–898.

50. van Ooij P, Markl M, Collins JD, et al. Aortic valve stenosis alters expression of regional aortic wall shear stress: New insights from a 4-dimensional flow magnetic resonance imaging study of 571 subjects. *J Am Heart Assoc* 2017;6:e005959.
51. von Knobelsdorff-Brenkenhoff F, Karunaharamoorthy A, Trauzeddel RF, et al. Evaluation of aortic blood flow and wall shear stress in aortic stenosis and its association with left ventricular remodeling. *Circ Cardiovasc Imaging* 2016;9:e004038.
52. van Kesteren F, Wollersheim LW, Baan J, et al. Four-dimensional flow MRI of stented versus stentless aortic valve bioprostheses. *Eur Radiol* 2017;1–8.
53. von Knobelsdorff-Brenkenhoff F, Trauzeddel RF, Barker AJ, et al. Blood flow characteristics in the ascending aorta after aortic valve replacement—a pilot study using 4D-flow MRI. *Int J Cardiol* 2014;170:426–433.
54. Harris AW, Krieger E V, Kim M, et al. Cardiac magnetic resonance imaging versus transthoracic echocardiography for prediction of outcomes in chronic aortic or mitral regurgitation. *Am J Cardiol* 2017 Apr;119:1074–1081.
55. Myerson SG, d'Arcy J, Mohiaddin R, et al. Aortic regurgitation quantification using cardiovascular magnetic resonance: association with clinical outcome. *Circulation* 2012 Sep;126:1452–1460.
56. Ribeiro HB, Orwat S, Hayek SS, et al. Cardiovascular magnetic resonance to evaluate aortic regurgitation after transcatheter aortic valve replacement. *J Am Coll Cardiol* 2016;68:577–585.
57. Chelu RG, van den Bosch AE, van Kranenburg M, et al. Qualitative grading of aortic regurgitation: a pilot study comparing CMR 4D flow and echocardiography. *Int J Cardiovasc Imaging* 2016;32:301–307.
58. Ewe SH, Delgado V, Van Der Geest R, et al. Accuracy of three-dimensional versus two-dimensional echocardiography for quantification of aortic regurgitation and validation by three-dimensional three-directional velocity-encoded magnetic resonance imaging. *Am J Cardiol* 2013;112:560–566.
59. Uretsky S, Argulian E, Narula J, Wolff SD. The present and future use of cardiac magnetic resonance imaging in assessing mitral regurgitation: current evidence. *J Am Coll Cardiol* 2018;71:547–563.
60. Biner S, Rafique A, Rafii F, et al. Reproducibility of proximal isovelocity surface area, vena contracta, and regurgitant jet area for assessment of mitral regurgitation severity. *JACC Cardiovasc Imaging* 2010;3:235–243.
61. Uretsky S, Gillam L, Lang R, et al. Discordance between echocardiography and MRI in the assessment of mitral regurgitation severity: a prospective multicenter trial. *J Am Coll Cardiol*. 2015;65:1078–1088.
62. Fujita N, Chazouilleres AF, Hartiala JJ, et al. Quantification of mitral regurgitation by velocity-encoded cine nuclear magnetic resonance imaging. *J Am Coll Cardiol* 1994;23:951–958.
63. Myerson SG, D'Arcy J, Christiansen JP, et al. Determination of clinical outcome in mitral regurgitation with cardiovascular magnetic resonance quantification. *Circulation* 2016;133:2287–2296.
64. Penicka M, Vecera J, Mirica DC, Kotrc M, Kockova R, Van Camp G. Prognostic implications of magnetic resonance — derived quantification in asymptomatic patients with organic mitral regurgitation: comparison with Doppler echocardiography-derived integrative approach. *Circulation* 2017;CIRCULATIONAHA.117.029332.
65. Dyverfeldt P, Kvitting JPE, Carlhäll CJ, et al. Hemodynamic aspects of mitral regurgitation assessed by generalized phase-contrast MRI. *J Magn Reson Imaging* 2011;33:582–588.
66. Al-Wakeel N, Fernandes JF, Amiri A, et al. Hemodynamic and energetic aspects of the left ventricle in patients with mitral regurgitation before and after mitral valve surgery. *J Magn Reson Imaging* 2015;42:1705–1712.
67. Witschey WRT, Zhang D, Contijoch F, et al. The influence of mitral annuloplasty on left ventricular flow dynamics. *Ann Thorac Surg* 2015;100:114–121.
68. Podlesnikar T, Delgado V, Bax JJ. Cardiovascular magnetic resonance imaging to assess myocardial fibrosis in valvular heart disease. *Int J Cardiovasc Imaging* 2018;34:97–112.
69. Messroghli DR, Moon JC, Ferreira VM, et al. Clinical recommendations for cardiovascular magnetic resonance mapping of T1, T2, T2\* and extracellular volume: A consensus statement by the Society for Cardiovascular Magnetic Resonance (SCMR) endorsed by the European Association for Cardiovascular Imag. *J Cardiovasc Magn Reson* 2017;19:75.
70. Azevedo CF, Nigri M, Higuchi ML, et al. Prognostic significance of myocardial fibrosis quantification by histopathology and magnetic resonance imaging in patients with severe aortic valve disease. *J Am Coll Cardiol* 2010;56:278–287.
71. Lee H, Park J-B, Yoon YE, et al. Noncontrast myocardial T1 mapping by cardiac magnetic resonance predicts outcome in patients with aortic stenosis. *JACC Cardiovasc Imaging* 2017;1–10.
72. Gaasch WH, Aurigemma GP. Inhibition of the renin-angiotensin system and the left ventricular adaptation to mitral regurgitation. *J Am Coll Cardiol* 2002;39:1380–1383.
73. Perazella MA, Setaro JF. Renin-angiotensin-aldosterone system: Fundamental aspects and clinical implications in renal and cardiovascular disorders. *J Nucl Cardiol* 2003;10:184–196.
74. Messroghli DR, Radjenovic A, Kozerke S, Higgins DM, Sivananthan MU, Ridgway JP. Modified Look-Locker inversion recovery (MOLLI) for high-resolution T1 mapping of the heart. *Magn Reson Med* 2004;52:141–146.
75. McDiarmid AK, Swoboda PP, Erhayiem B, et al. Single bolus versus split dose gadolinium administration in extra-cellular volume calculation at 3 Tesla. *J Cardiovasc Magn Reson* 2015;17:6.
76. Schelbert EB, Testa SM, Meier CG, et al. Myocardial extravascular extracellular volume fraction measurement by gadolinium cardiovascular magnetic resonance in humans: slow infusion versus bolus. *J Cardiovasc Magn Reson* 2011;13:16.
77. White SK, Sado DM, Fontana M, et al. T1 mapping for myocardial extracellular volume measurement by CMR. *JACC Cardiovasc Imaging* 2013;6:955–962.
78. Wong TC, Piehler K, Meier CG, et al. Association between extracellular matrix expansion quantified by cardiovascular magnetic resonance and short-term mortality. *Circulation* 2012;126:1206–1216.
79. Milano AD, Faggian G, Dodonov M, et al. Prognostic value of myocardial fibrosis in patients with severe aortic valve stenosis. *J Thorac Cardiovasc Surg* 2012 Oct;144:830–837.
80. Dweck MR, Joshi S, Murigu T, et al. Midwall fibrosis is an independent predictor of mortality in patients with aortic stenosis. *J Am Coll Cardiol* 2011 Sep;58:1271–1279.
81. Mewton N, Liu CY, Croisille P, Bluemke D, Lima JAC. Assessment of myocardial fibrosis with cardiovascular magnetic resonance. *J Am Coll Cardiol* 2011;57:891–903.
82. Cavalcante JL, Rijal S, Abdelkarim I, et al. Cardiac amyloidosis is prevalent in older patients with aortic stenosis and carries worse prognosis. *J Cardiovasc Magn Reson* 2017;19:98.
83. Lee S-P, Lee W, Lee JM, et al. Assessment of diffuse myocardial fibrosis by using MR imaging in asymptomatic patients with aortic stenosis. *Radiology* 2015 Feb;274:359–369.
84. Sado DM, White SK, Piechnik SK, et al. Identification and assessment of Anderson-Fabry disease by cardiovascular magnetic resonance noncontrast myocardial T1 mapping. *Circ Cardiovasc Imaging* 2013;6:392–398.
85. Bull S, White SK, Piechnik SK, et al. Human non-contrast T1 values and correlation with histology in diffuse fibrosis. *Heart* 2013;99:932–937.
86. Sparrow P, Messroghli DR, Reid S, Ridgway JP, Bainbridge G, Sivananthan MU. Myocardial T1 mapping for detection of left ventricular myocardial fibrosis in chronic aortic regurgitation: pilot study. *AJR Am J Roentgenol* 2006;187:W630–635.
87. Edwards NC, Moody WE, Yuan M, et al. Quantification of left ventricular interstitial fibrosis in asymptomatic chronic primary degenerative mitral regurgitation. *Circ Cardiovasc Imaging* 2014;7:946–953.



88. Van De Heyning CM, Magne J, Piérard LA, et al. Late gadolinium enhancement CMR in primary mitral regurgitation. *Eur J Clin Invest* 2014;44:840–847.
89. Flett AS, Sado DM, Quarta G, et al. Diffuse myocardial fibrosis in severe aortic stenosis: an equilibrium contrast cardiovascular magnetic resonance study. *Eur Heart J Cardiovasc Imaging* 2012;13:819–826.
90. Geiger J, Rahsepar AA, Suwa K, Powell A, Ghasemiesfe A, Barker AJ, et al. 4D flow MRI, cardiac function, and T<sub>1</sub>-mapping: Association of valve-mediated changes in aortic hemodynamics with left ventricular remodeling. *J Magn Reson Imaging*. 2017 Dec.
91. Van Ooij P, Allen BD, Contaldi C, et al. 4D flow MRI and T1-mapping: Assessment of altered cardiac hemodynamics and extracellular volume fraction in hypertrophic cardiomyopathy. *J Magn Reson Imaging* 2016;43:107–114.
92. Kalam K, Otahal P, Marwick TH. Prognostic implications of global LV dysfunction: a systematic review and meta-analysis of global longitudinal strain and ejection fraction. *Heart* 2014;100:1673–1680.
93. Witkowski TG, Thomas JD, Debonnaire PJMR, et al. Global longitudinal strain predicts left ventricular dysfunction after mitral valve repair. *Eur Heart J Cardiovasc Imaging* 2013;14:69–76.
94. Mentias A, Naji P, Gillinov M, et al. Baseline LV strain independently predicts exercise capacity in asymptomatic primary mitral regurgitation patients and preserved LV ejection fraction undergoing rest-stress echocardiography. *Eur Heart J* 2016;37:1238–1239.
95. Ahmed MI, Gladden JD, Litovsky SH, et al. Increased oxidative stress and cardiomyocyte myofibrillar degeneration in patients with chronic isolated mitral regurgitation and ejection fraction >60%. *J Am Coll Cardiol* 2010;55:671–679.
96. Schiros CG, Dell'Italia LJ, Gladden JD, et al. Magnetic resonance imaging with 3-dimensional analysis of left ventricular remodeling in isolated mitral regurgitation: Implications beyond dimensions. *Circulation* 2012;125:2334–2342.
97. Ewe SH, Haeck MLA, Ng ACT, et al. Detection of subtle left ventricular systolic dysfunction in patients with significant aortic regurgitation and preserved left ventricular ejection fraction: speckle tracking echocardiographic analysis. *Eur Heart J Cardiovasc Imaging* 2015;16:992–999.
98. Park SH, Yang YA, Kim KY, et al. Left ventricular strain as predictor of chronic aortic regurgitation. *J Cardiovasc Ultrasound* 2015;23:78–85.
99. Di Salvo G, Rea A, Mormile A, et al. Usefulness of bidimensional strain imaging for predicting outcome in asymptomatic patients aged ≤ 16 years with isolated moderate to severe aortic regurgitation. *Am J Cardiol* 2012;110:1051–1055.
100. Kearney LG, Lu K, Ord M, et al. Global longitudinal strain is a strong independent predictor of all-cause mortality in patients with aortic stenosis. *Eur Heart J Cardiovasc Imaging* 2012;13:827–833.
101. Yingchoncharoen T, Gibby C, Rodriguez LL, Grimm RA, Marwick TH. Association of myocardial deformation with outcome in asymptomatic aortic stenosis with normal ejection fraction. *Circ Cardiovasc Imaging* 2012;5:719–725.
102. Dahl JS, Videbæk L, Poulsen MK, Rudbæk TR, Pellikka PA, Maller JE. Global strain in severe aortic valve stenosis relation to clinical outcome after aortic valve replacement. *Circ Cardiovasc Imaging* 2012;5:613–620.
103. Obokata M, Nagata Y, Wu VCC, et al. Direct comparison of cardiac-magnetic resonance feature tracking and 2D/3D echocardiography speckle tracking for evaluation of global left ventricular strain. *Eur Heart J Cardiovasc Imaging* 2016;17:525–532.
104. Schuster A, Stahnke VC, Unterberg-Buchwald C, et al. Cardiovascular magnetic resonance feature-tracking assessment of myocardial mechanics: Intervendor agreement and considerations regarding reproducibility. *Clin Radiol* 2015;70:989–998.